Multielemental analysis of Antarctic soils using Calibration Free Laser-Induced Breakdown Spectroscopy

Jesús M. Anzano[1*], Andrés Cruz-Conesa[1], Roberto-J. Lasheras[1], César Marina-Montes[1], Luis-Vicente Pérez-Arribas[2], Jorge O. Cáceres[2], Abrahan I. Velásquez[1,3] and Vincenzo Palleschi[4]

[1]Laser lab, Chemistry & Environment Group, Department of Analytical Chemistry, Faculty of Sciences, University of Zaragoza. Pedro Cerbuna 12, 50009-Zaragoza, Spain

[2] Laser Chemistry Research Group, Department of Analytical Chemistry, Faculty of Chemistry, Complutense University of Madrid. Plaza de Ciencias 1, 28040-Madrid, Spain

[3]Faculty of Agricultural Sciences, University Laic Eloy Alfaro of Manabí, 12th Street, 130214 Manta, Ecuador.

[4]Laboratory of Applied and Laser Spectroscopy, ICCOM/CNR, Via G. Moruzzi, 1, Pisa 56124, Italy

Abstract: Laser-induced breakdown spectroscopy (LIBS) is a quick technique that allows the analysis of all types of samples without destroying them and with much reduced sample treatment. One of its many applications is the study of geological samples such as soils. Because of the complexity of the matrix, it is very difficult to find or manufacture standards for these types of samples. Therefore, a good alternative is to make use of a methodology, called Calibration Free (CF), where instead of using standards, the physical parameters of the plasma created by the interaction of the laser with the sample are studied and related to the elements and species that compose it. This methodology is followed to perform a multielemental quantitative analysis of soil samples from Antarctica. Two studies were made, differing in the optimization of the instrumental parameters in order to obtain the best possible spectra in the chosen spectral lines. In both cases, the signal to noise ratio (SNR) was used to evaluate the quality of the spectra, but in the second study a full factorial design 2^3 with center and axial points was developed to get better results. The choice of spectral lines was based on a series of criteria, being stricter in the second study. The samples were mainly composed of the following oxides: SiO_2, Al_2O_3, Fe_2O_3, CaO, MgO, Na_2O, TiO and K_2O. In the second study, it was also possible to determine the species present in lower concentrations: Mn, Cr, V, Sr, Zr, BA and Li. The results were compared with those provided by ICP-OES analysis, obtaining close values for most oxides, especially in the second study. For minority elements, the CF-LIBS and the ICP-OES results were within the same order of magnitude in all cases except the Cr case. These results show that CF-LIBS can be very useful in the characterization of complex samples from remote regions, such as Antarctic soils.

Keywords: LIBS; Calibration-free LIBS; Soil; Antarctica

*: janzano@unizar.es

1. Introduction

LIBS is a suitable technique to analyze soil samples. The speed at which LIBS obtains the emission spectra enables a large quantity of information to be gathered in a matter of seconds. These spectra range from 250 to 900 nm, approximately, so that most of the elements in the samples can be identified. The minimal sample preparation required reduces the time spent and the cost of the analysis of these types of samples which usually have to be dissolved using aggressive substances for analysis by other techniques. In addition, LIBS can perform in situ analysis using portable LIBS devices. The amount of sample that LIBS needs is minimal, only pg or ng are lost in each laser pulse. For this reason, it can be considered a micro-destructive technique. Another property of this technique which makes it suitable for characterizing soils is the possibility of creating the composition and depth profiles of the samples [1,2].

The knowledge of the composition of a soil is very important because it allows solving problems related to its origin, classifying it or even dating it. The elements found in soils can offer prints about possible deposits, or can serve as a base for studies that relate the presence of any sample substances together with their transport mechanisms and their impact on the environment [3,4]. For this last reason, it is important to analyze the soil from the Antarctic Region which in principle should not be contaminated by human activity. It is useful to compare the presence of metals in the soil and, for example, the presence of metals in atmospheric aerosols. If the metals present in the air are not in the soil, this may signify that these metals have an external origin, probably coming from other areas of the planet carried by the winds. LIBS has been employed to analyze soil components on several occasions. Harmon et al. and McMillan et al. summarized the application of LIBS for the analysis of geological samples, including soils [2,4]. Diaz et al. evaluated total element concentrations in mixtures of soils and fertilizers by calibration curves [5]. Dell'Aglio et al. made a quantitative analysis of Cr, Cu, Pb, V, and Zn in different soil samples drawing a calibration line for each element, and plotting the intensity of a given emission line as a function of the concentration determined by ICP-OES [6]. Kim et al. used LIBS coupled with a chemometric method to rapidly discriminate between clean soils and soils contaminated with heavy metals or oils [7]. Popov et al. tried to improve analytical figures-of-merit of the single-pulse LIBS for the determination of trace elements in soil samples [8]. Senesi et al. made a review of the quantitative analyses of carbon and organic carbon in soils [9].

The main problem for performing quantitative analysis by LIBS is the matrix effect. It is very difficult to obtain or buy standards of soil samples that allow creating calibration lines because of the character of the plasma and the behavior of the atoms depend on many variables related to the origin of the ablated material: composition, crystallinity, optical reflectivity, optical transmissivity and morphology of the surface [2]. Other problems that can appear are the lack of sensitivity to be able to quantify elements in very low concentrations and the representativeness of the measurements if the sample has a high degree of heterogeneity [10].

As a solution to the matrix effect limitation, in 1999 a new method called Calibration Free (CF or CF-LIBS) was developed. This method measures the physical parameters of the plasma, and performs a quantitative and multielemental analysis without having to prepare any type of pattern [11]. This methodology has been used in various works for several types of samples,

such as soils [11,12], rocks [13,14], sands [15], metal-alloys [16,17], precious alloys [18], glass [19], steel [20], coral skeletons [21] and industrial wastes [22].

There are different ways to apply CF-LIBS. In this work, a CF-LIBS method [23, 24] based in the condition of a plasma in local thermal equilibrium [25] is carried out with the purpose of demonstrating that CF-LIBS could be a good option for obtaining quantitative multielemental information from soil samples. Two different analyses were made. In the first one, we sought to test whether promising results could be obtained quickly using this methodology in such a complex sample. Once the results of the first experiment were known, a second analysis was made. Here, we used more samples and put more emphasis on the optimization of the instrumental parameters and the spectra and in the selection of the spectral lines included in the calculations.

2. Experimental

2.1. Samples

Soil samples were collected at different locations on Deception Island (62°58'09"S, 60°42'33"W) during the 2017/2018 & 2018/2019 Spanish Antarctic research campaigns. This island is the caldera of an active volcano, being part of the South Shetland Islands (Antarctica). Researchers were based at the Spanish Antarctic Research Station "Gabriel de Castilla".

The first analysis was applied on a soil sample collected in the Antarctic campaign 2017/18 in Bahía Puerto Foster (62°58'38"S, 60°40'33"O). For the second analysis, six different soil samples were analyzed. These samples were collected in the Antarctic campaign 2018/19. The soils were labeled with the name of their place of origin and its coordinates: Punta Descubierta (PD) (62.59.431 S, 60.43.361 O); Pingüinera Punta (PP) (62.59.977 S, 60.33.364 O); Depósito Balleneros (DB) (62.58.722 S, 60.33.690 O); Playa Fumarolas (PF) (62.57.847 S, 60.42.851 O); Playa Lobera (PL) (62.59.880 S, 60.34.571 O) and Captador Grande (CG) (62.58.631 S, 60.40.448 O).

The adequacy of the sample was different from the first experiment. The particle size of the soil samples was reduced with a mortar. Approximately 200 mg of soil samples was weighed and compressed using a manual hydraulic press (Perkin Elmer IR Accessory, Hydraulic Press) with $10x10^4$ N for 2 min, to obtain pellets for LIBS analysis.

2.2. LIBS instrumentation

The experimental set-up is based on a Q-switched Nd:YAG laser (BrilliantQuantel, model Ultra CFR) with a wavelength of 1064 nm, a pulse duration around 8 ns and a pulse energy maximum of 50 mJ. The sample was placed in a sample chamber that allows working in an argon atmosphere. The focal length was 7.7 cm. The light emitted by the plasma was collected by optic fibers connected to an Echelle spectrometer (Andor Mechelle ME5000, 195 mm focal length, F/7, l/Al 5000). The spectrometer has an intensified CCD detector (Andor iStar DH734, 1024 ×

1024 pixels, 13,6 × 13,6 μm^2 by pixel, 18 mm of intensifier diameter). The spectrometer and detector were calibrated with a mercury argon lamp. All the spectra were taken in an argon atmosphere in order to avoid atmospheric contamination in trace detection

For the analysis of the 2017/18 sample, we applied CF-LIBS to six spectra. Each spectrum was the accumulation of 15 measurements at different points of the sample. From the six spectra, we obtained the average value and the standard deviation of the sample components. For the analysis of each of the 2018/19 samples we again applied CF-LIBS to six spectra. In this case, each one of these spectra was the average of two spectra formed from the accumulation of 60 measurements made in different regions of the pellet.

To perform the treatment of the spectra and to apply CF-LIBS, the software LIBS++ developed by Ciucci et al. was employed. [26]

2.3 Instrumental parameters optimization

The parameters studied were laser beam energy, time of delay and integration time to obtain the best possible signals in the spectra.

In the first study, we selected some spectral lines of the elements of interest and tested different times and energies. The parameter selection was based on the signal-noise ratios (SNR) [27] that these lines offered. The possible interaction between the variables and the SNR were not considered.

For the second study, a more sophisticated method was used to optimize the instrumental parameters and to improve the spectra collected. It consisted in a central composite design for two levels and three factors. The variables evaluated were as follows: delay time at five levels (10, 300, 900, 1500 and 1910 ns), gate width at five levels (320, 1000, 2000, 3000 and 3680 ns) and laser pulse energy at five levels (22.5, 25, 35, 45 and 50 mJ). The variable levels were coded between -1.68 (lower level) and +1.68 (higher level), with the central point (0) used to calculate experimental errors (Table 1). The Playa Fumarolas sample was used to optimize the instrumental conditions in the CF-LIBS analyses. Two spectra were averaged for each one of the 19 experiments. Each spectrum was the accumulation of 40 measurements made in different regions of the pellet.

The SNR calculated for the following lines were used as responses of the factorial design: SI I (288.15), Al I (394.41), Ca I (422.7), Ca II (317.96), Fe I (361.87), Fe II (239.55), Mg I (518.37), Mg II (279.07), Ti I (337.33) and Ti II (453.47). The lines selected were those of the major elements present in the sample, both in the neutral state and the first ionization, trying to cover the maximum wavelength range of the spectrum. A mathematical approach developed by Derringer and Suich [28] based on desirability functions applied to optimize multi-response experiments was used in this study.

2.4. FESEM instrumentation

Field emission scanning electron microscopy (FESEM) was employed for the initial morphological study of the material of the first sample. Compared with conventional SEM, FESEM produces clearer, less electrostatically distorted images with spatial resolution three to

six times better [29]. The Merlin Field emission scanning electron microscopy (FESEM) was used for calculating the crater diameters formed by the laser beam over the surface of the soil sample, which is a parameter necessary to quantify the laser intensity or irradiance. This analysis was performed by the General Services Research Support of University of Zaragoza. A thin layer of conductor platinum was arranged over the soil sample under vacuum conditions (10^{-7} mbar). A secondary electron detector (SE2) and a backscattered electron detector (AsB) were employed. A cobalt filter was used for calibration and the accelerating voltage was set to 1 KV. A magnification range from 100 to 10000 was studied.

3. Results and discussion

FESEM analysis allowed us to obtain the size of the crater. As shown in Figure 1, the soil surface is practically homogeneous with small indentations. This proves that the sample preparation was a good option to have a surface where the shot-to-shot variability should not initially be too high. The crater diameter can be seen in the same figure. The laser energy used of 45 mJ and a pulse duration of 7.7 ns result in a power of 5.84 MW. With this value and the crater radius which reached 232.25 µm, the irradiance obtained was 2.52 GW/cm^2.

3.1. Instrumental parameters optimization

From the first study, it was deduced that when delay times lower than 300 ns are used, the peaks suffer from poor resolution because there is a lot of noise. This noise is due to the continuous emission that occurs in the first states of the plasma when the electron density is very high. With times higher than 3000 ns, the intensity of the peaks is too low. Integration times lower than 1000 ns provided a low sensitivity and times higher than 5000 ns induced a large amount of noise.

For the first study, the following parameter values were chosen: an energy of 45 mJ, a delay time of 500 ns and an integration time of 2000 ns.

For the second study, the individual desirability of each monitored line was calculated. This consisted in converting each response into an individual desirability value (di), which ranges between $0 \leq d_i \leq 1$ where di =1 corresponds to a desired response, with the highest SNR, while di=0 would be an undesired response with the lowest SNR. Subsequently the individual desirability values were combined using the arithmetic mean to obtain a single response for each experiment. This value is called the overall desirability (OD). The OD value of each experiment appears in Table 1.

The goal of this approach is to obtain a model based on the calculated OD to determine the best description of the experimental region. The quality of the model was evaluated through analysis of variance (ANOVA).

The value of the energy and the interactions between variables were not significant at the 95 % confidence level, according to the analysis because of that we selected a value (45 mJ) close to the maximum possible, thus trying to increase the sensitivity to detect elements in lower concentrations. The coefficients of delay time and gate width were valid and served to build a model that would allow us to predict the OD. The model constructed was as follows:

$$OD = 0.57 + 0.23\ DT + 0.13\ GW \quad (1)$$

Where the delay time (DT) and the gate width (GW) have to be introduced in normalized form. Based on this model, a response surface was built (Figure 2). The OD value grows as the delay time increases faster than the gate width increases. The darkest area represents the combination of delay times and gate widths, which produce the maximum OD value. Although theoretically the OD cannot be higher than one on the surface, there are higher values due to the prediction error in the model.

In summary, it is better to use high values of delay time and gate width. We tested using higher values than those that served to create the model, but the SNR were not better in general. Moreover, if the delay time is too high it could mean a lower electron density in the plasma that would invalidate the Mc. Whirther criterion and would not allow supposing a plasma in local thermal equilibrium. We therefore decided to employ a delay time of 1900 ns and a gate width of 3650 ns.

3.2. Element identification and choice of analytical lines

The metals from the first sample that were clearly identified were Fe, Ca, Si, Mg, Al, Ti, Na, and K. In the second experiment, in addition to these it was possible to find emission lines of minor elements. The higher quality of the spectra due to the optimization and to the major number of measurements that give place to the final spectrum, allowed differentiating their emission lines from noise. Figure 3 shows the spectrum of the Playa Fumarolas sample with some spectral lines identified.

The spectra of the different samples were very similar, changing only the intensity of the peaks or the related intensity between ones and others. Fe and Ti were the elements that presented a larger number of signals from both the neutral and the ionized species. Ca was also a rich element while Mg presented fewer lines. Al and especially K and Na have very few lines with a relative intensity that allows observing them by LIBS. We did not find transitions that involve the ion of any of these three elements. Finally, Si gave rise to a several lines of the excited species but very few of the ionized.

As previously mentioned, not all the lines found can be used in the calculation. We paid attention to a series of rules. The lines that surround the ground state together with the lines corresponding to transitions with the lowest levels of energy below 6000 cm^{-1} were excluded because they are susceptible to self-absorption. The lines with a spontaneous emission coefficient lower than 2×10^6 s^{-1} were not taken because in these cases the emission time could be comparable to the time associated with plasma variations losing the homogeneity during the measurement. As far as possible, the emission lines with very high relative intensity were excluded because the spatial integration of the emission signal along the optical path can overestimate its area [30]. Neither is it possible to use the lines that offer a very low SNR, those that are very wide, those that include more than one state of the same element, or those that suffer spectral interferences.

For not fulfilling these conditions, several of the lines that had been initially identified were removed, especially the titanium, iron and magnesium lines. The lines finally used for the determination of Antarctic soils by LIBS-CL in the first experiment are found in Table 2.

In the second experiment, in addition to following these rules the line selection was refined. Some lines were added while others were removed in order to achieve an R^2value higher than 0.99 in the Saha-Boltzman straight lines from which the temperature value is extracted. These straight lines should also have a similar slope. Table 2 shows the lines used in the calculation for all the samples of the Antarctic Campaign 2018/19.

3.3. Electron density and plasma temperature

The electronic density is determined from the hydrogen line that appears at 656,28 nm [31]. Table 4 contains the electronic density values of all the analyzed samples.

As already stated, McWhirter's criterion is widely used to verify that the plasma is in LTE. This is because in LTE the excitation processes due to collisions must predominate over the radiative [25]. This can be checked using equation (2).

$$N_e\ (cm^{-3}) \geq 1.6 \times 10^{12}\ T_e^{1/2} (\Delta E)^3 \quad (2)$$

Here, Ne (cm^{-3}) is the electron density, T (K) is the plasma temperature and ΔE (eV) is the difference between neighboring states with the allowed transition.

The criterion is fulfilled for the elements considered both in neutral and ionized state. For example, the transition of Fe I 3p63d64s2 – 3p63d6(5D)4s4p(3P0) has a ΔE = 3.2 eV and the transition of Fe II 3d6(5D)4s – 3d6(5D)4p has a ΔE = 4.8 eV. As will be seen later, for the first study a temperature of around 11300 K is obtained and for the second all the samples provide values around 9000 K. Equation 2 provide N_e limit values of 5.6×10^{15} cm^{-3} for Fe I and 1.9×10^{16} cm^{-3} for Fe II in the first case and values of 5.0×10^{15} cm^{-3} for Fe I and 1.8×10^{16} cm^{-3} for Fe II in the second. The values of Ne that we obtained experimentally were clearly higher, so that LTE is verified.

The Saha-Boltzmann plot was constructed (Figure 4) from Fe, Ca and Ti lines. For each spectrum, the intensity and the spectral parameters of the lines are introduced together with the calculated value of electronic density. These three elements are those, which present the most emission lines, both in the spectra and in the set of lines finally used in the representation. Therefore, their weight is very high. The lines of the other elements are minor in number, thus the overestimation or underestimation of the intensity of any line would have a much greater effect on the temperature estimation obtaining less reliable values. Due to this fact, the slope of the straight lines of the other elements were neglected.

In the Saha-Boltzmann plot corresponding to the Playa Fumarolas sample (Figure 4), there is a series of points. Those on the right correspond to the transitions that involve the single ionized elements and those on the left correspond to the neutral. It can be appreciated how all the points are distributed giving rise to straight lines with high R^2values and with slopes very close to each other. The Saha-Boltzmann plots of the other samples were constructed with the same lines and in all cases, high R^2 values and similar slopes were obtained. The straight lines emerging from the first experiment did not have such high R^2values and the points in Saha-Boltzmann plot were more scattered.

The temperature values obtained averaging the value of the three slopes for each sample are presented in Table 3. The errors are extracted from the standard deviation of the values generated by each one of the six spectra treated for each sample. The difference in both the T_e and N_e values is within the errors bars between the samples collected at different points. This indicates that the morphology and composition of the soil should not be very different. However, the temperature is considerably higher in the 2017/18 soil sample, most probably because the delay time used for the spectra collection was 500 ns while for the other samples the spectra was 2000 ns. It is confirmed that the plasma temperature is higher in the first moments after it is formed and then rapidly begins to cool [32]. The same occurs with the electronic density.

3.4. Sample composition

In order to obtain quantitative results for the components of the soil, the concentrations of the different species detected were calculated by the intercepts q_s derived from the linear regressions of the corresponding Saha-Boltzmann plots carried out with a fixed slope, $m=-1/kT_e$.

Table 4 shows the major constituents of the Antarctic soil samples. The results are given in mass percentages of the oxides. This is the way in which the elements are present in the soil sample. Exhibiting the results in the form of oxides is common and the most widespread way when soils or rocks are analyzed. The error bars shown are calculated from the standard deviation of the component values obtained by applying CF-LIBS to each one of the six spectra. The first sample was analyzed previously by ICP-OES by CSIC in Barcelona. The results have been taken as a reference to test how good the performance of the CF-LIBS method is.

The CF-LIBS analysis of the 2017/18 soil sample presents the greatest differences compared with the reference analysis for sodium oxide, silica and titanium oxide. In the first two cases, CF- LIBS provides much lower concentrations. Sodium has only three signals; two with a very high relative intensity that also belong to the ground state. The probability that these lines suffer self-absorption processes is therefore considerable. In the case of silica, it is possible that as silicon is the major component of the sample, the signals of the element could be saturated and therefore they would not be able reach the intensity that they should. The sum of all the oxides determined by LIBS gives rise to only 80.71%, and it is logical to think that what is missing to reach 100% is mostly the undetected silica. The difference practically coincides with the amount of SiO_2 missing to match the amount obtained by the reference analysis.

The samples of the Antarctic campaign 2018/19 do not show this problem with the silica. It is probably that the better optimization of the spectra and the greater care in the selection of the analytical lines made that the Si lines had now their correct intensity. The rest of the oxide concentrations are closer to those provided by the ICP-OES, but the TiO_2 percentage is still too high. Despite being in low concentrations, Ti signals in the spectra showed a high intensity. This may be a consequence of the low sensitivity of titanium spectral lines having a high relative intensity compared to the lines of other elements.

The composition of the different samples was similar, as would be expected due to the volcanic origin of the island. Samples taken on beaches (PF and PL) differed from the rest in their composition, possibly due to the proximity to the sea and the greater human activity in these areas compared to more inland areas of the island.

The CF-LIBS results for minority elements (Table 5) are within the expected range if we take into account the concentrations provided by ICP. It could be said that in all cases except for the chrome case they are within the same order of magnitude. Again, the elevated relative intensity could be the reason for this overestimation. The higher uncertainty in the measurements is normal for elements in low concentrations since only a few spectral lines for each one could be clearly identified. The difference between samples could indicate an enrichment of some of the metals in some areas of Deception Island, but the high uncertainty and the absence of a reference analysis of each of the samples does not allow such a hypothesis to be confirmed.

4. Conclusions

A CF-LIBS method was put into practice to obtain quantitative results of the composition of Antarctic soil samples. The selection of the analytical lines can be considered the most critical step in the CF-LIBS method. Therefore, obtaining spectral lines of high intensity and free from interference and self-absorption turns out to be a key aspect. This task is easier, as demonstrated in this work, when an optimization of instrumental parameters such as the energy pulse, integration time or delay time is carried out. Surely, delay time is the most important variable to optimize because, as has been shown, it considerably influences the plasma electronic density and temperature values. The optimization and the selection of spectral lines made in this work allows an accurate determination of the major oxides that make up the Deception Island soils through a simple CF-LIBS method. The composition was similar in the different locations of the island although small differences were found in the samples taken on beaches.

This method is also capable of detecting and estimating the concentration of minor constituents in soils, but the accuracy and the precision shown in this work are possibly too low in order to consider using a CF-LIBS method as a good option for reference determination. More work is necessary on the use of CF-LIBS and the LIBS technique particularly to produce accurate determinations of elements in low concentrations, especially in complex matrices. The lack of sensibility has always been a drawback of LIBS. Nevertheless, the method shown in this work may be very interesting for a rapid or in-situ analysis of soils giving a first approximation of what the soil contains, thus avoiding sampling and ICP analysis after sample treatment of soils that are not of interest due to their content. The CF-LIBS method certainly has the advantage of not having to dissolve the samples or use standards. When the method is optimized, simply taking the spectra of a new sample with the same instrumental parameters would allow obtaining its composition immediately. This work opens up the possibility for our group to send LIBS instrument to the Antarctic Region in future campaigns to measure the soils in real time, allowing the detection of pollution from trace elements.

Acknowledgments

The authors gratefully acknowledge the Government of Aragon, Universidad de Zaragoza, the European Social Fund Proposal E49_20R and the Ministry of Science, Innovation and Universities of Spain (CTM2017-82929-R). Authors would like to acknowledge the use of Servicio General de Apoyo a la Investigación-SAI, University of Zaragoza. The authors also thank the military staff at the Gabriel de Castilla Spanish Antarctic Research Station and Javier del Valle Melendo (Centro Universitario de la Defensa- University of Zaragoza) for help with the sample collection and installation of the equipment.

References

[1] Musazzi, S.; Perini, U. In *Laser-Induced Breakdown Spectroscopy Theory and Applications*, Musazzi, s.; Perini, U., Eds; Springer Series in Optical Sciences 182; Springer: New York, **2014**, 59-61.

[2] Harmon, R. S.; Russo, R. E.; Hark, R.R. Applications of laser-induced breakdown spectroscopy for geochemical and environmental analysis: A comprehensive review. *Spectrochim. Acta, Part B*. **2013**, 87, 11–26.

[3] Godal, M.A.; Dastageer, M.A. In Laser-Induced Breakdown Spectroscopy Theory and Applications, Musazzi, s.; Perini, U., Eds; Springer Series in Optical Sciences 182; Springer: New York, **2014**, 293-306.

[4] McMillan, N. J.; Rees, S.; Kochelek, K.; McManus, C. Geological Applications of Laser-Induced Breakdown Spectroscopy. *Geostan. Geoanal. Res*. **2014**, 38(3), 329-343.

[5] Díaz, D.; Hahn, D.W.; Molina, A. Evaluation of Laser-Induced Breakdown Spectroscopy (LIBS) as a Measurement Technique for Evaluation of Total Elemental Concentration in Soils. *Appl. Spect.* **2012**, 66(1), 99-106.

[6] Dell'Aglio, M.; Gaudioso, R.; Senesi, G.S.; De Giacomo, A.; Zaccone, C.; Miano, T.M.; De Pascale, O. Monitoring of Cr, Cu, Pb, V and Zn in polluted soils by laser induced breakdown spectroscopy (LIBS). *J.Environ.Monit.* **2011**, 13, 1422-1426.

[7] Kim, G.; Kwak, J.; Kim, K.; Lee, H.; Kim, K,; Yang, H.; Park, K. Rapid detection of soils contaminated with heavy metals and oils by laser induced breakdown spectroscopy (LIBS). *J. Hazard Mater.* **2013**, 263(2), 754-760.

[8] Popov, A.M.; Colao, F.; Fantoni, R. Spatial confinement of laser-induced plasma to enhance LIBS sensitivity for trace elements determination in soils. *J.Anal. At. Spectrom.* **2010**, 25, 837-848.

[9] Senesi, G.S.; Senesi, N. Laser-induced breakdown spectroscopy (LIBS) to measure quantitatively soil carbon with emphasis on soil organic carbon. A review. *Anal. Chim. Acta* **2016**, 938, 7-17.

[10] Cremers, D. A.; Chinni, R.C.; Laser-Induced Breakdown Spectroscopy - Capabilities and Limitations. *Appl. Spectrosc. Rev.* **2009**, 44, 457–506.

[11] Herrera, K.; Tognoni, E.; Smith, B.W.; Omenetto, N.; Winefordner, J.D. Semiquantitative analysis of metal alloys, brass and soil samples by calibration-free laser-induced breakdown spectroscopy: recent results and considerations. *J. Anal. At. Spectrom.* **2009**, 24, 413–425.

[12] Pandhija, S.; Rai, N.K.; Rai, A.K.; Thakur S.N. Contaminant concentrations in envirommental samples using LIBS and CF-LIBS. *Appl. Phys. B.* **2010**, 98, 231.

[13] Rehan, I.; Kham, M.Z.; Reham, K.; Mateen, A.; Farooour, M.A.; Sultana, S.; Faroor, Z. Determination of toxic and essential metals in rock and sea salts using pulsed nanosecond laser-induced breakdown spectroscopy. *Appl. Opt*ics. **2018**, 57(2), 295-301.

[14] B. Sallé, J.L. Lacour, P. Mauchien, P. Fichet, S. Maurice, G. Manhes, Comparative study of different methodologies for quantitative rock analysis by laser-induced breakdown spectroscopy in a simulated Martian atmosphere. *Spectrochim. Acta Part B.* **2006,** 61, 301–314

[15] Díaz Pace, D.M.; Miguel, R.E.; Di Rocco, H.O.; García, F.A.; Pardini, L.; Legnaioli, S.; Lorenzetti, G.; Palleschi, V. Quantitative analysis of metals in waste foundry sands by calibration free-laser induced breakdown spectroscopy. *Spectrochim. Acta Part B*. **2017**, 131, 58-65.

[16] Shakeel, H.; Haq, S.U.; Aisha, G.; Nadeem, A. Quantitative analysis of Al-Si alloy using calibration free laser induced breakdown spectroscopy (CF-LIBS). *Phys Plasmas*. **2017**, 24, 1-7.

[17] Aguilera, J.A.; Aragón, C.; Cristoforetti, G.; Tognoni, E. Application of calibration-free laser-induced breakdown spectroscopy to radially resolved spectra from a copper-based alloy laser-induced plasma. *Spectrochim. Acta Part B*. **2009**, 64, 685-689.

[18] M.V. Belkov, V.S. Burakov, V.V. Kiris, N.M. Kozhukh, S.N. Raikov. Spectral standard free laser microanalysis of gold alloys. *J. Appl. Spectrosc.* **2005**, 72, 376–381.

[19] Gerhard, C.; Hermann, J.; Mercadier, L.; Loewenthal, L.; Axente, E.; Luculescu, C.R.; Sarnet, T.; Sentis, M.; Viöl, W. Quantitative analyses of glass via laser-induced breakdown spectroscopy in argon. *Spectrochim. Acta Part B.* **2014**, 101, 32-45.

[20] Shahm M.L.; Pulhani, A.K.; Gupta, G.P.; Suri, M. Quantitative elemental analysis of steel using calibration-free laser-induced breakdown spectroscopy. *Appl. Optics*. **2012**, 51(20), 4612-4621.

[21] Pandhija, S.; Rai, A.K. In situ multielemental monitoring in coral skeleton by CF-LIBS. *Appl. Physics B.* **2009**, 94(3), 545-552.

[22] Kumar, R.; Rai, A.K.; Alamelu, D.; Aggarwal, S.K. Monitoring of toxic elements present in sludge of industrial waste using CF-LIBS. *Environ. Monit. Assess*. **2013**, 185(1), 171-180.

[23] Ciucci, A.; Corsi, M.; Palleschi, V.; Rastelli, S.; Salvetti, A.; Tognoni, E. New procedure for quantitative elemental analysis by laser-induced plasma spectroscopy. *Appl. Spectrosc.* **1999**, 53, 960-964

[24] Tognoni, E.; Cristoforetti, G.; Legnaioli, S.; Palleschi, V. Calibration-Free Laser-Induced Breakdown Spectroscopy: State of the art. *Spectrochim. Acta Part B*. **2010**, 65, 1–14.

[25] Cristoforetti, G.; Giacomo, A.D.; Dell'Aglio, M.; Legnaioli, S.; Tognoni, E.; Palleschi, V.; Omenetto, N. Local Thermodynamic Equilibrium in Laser-Induced Breakdown Spectroscopy: Beyond the McWhirter criterion. *Spectrochim. Acta Part B*. **2010**, 65, 86-95.

[26] Ciucci, A.; Palleschi, V.; Rastelli, S.; Salvetti, A.; Singh, D. P.; Tognoni, E. CF-LIPS: a new approach to LIPS spectra analysis, *Laser Part. Beams*, **1999**, 17, 793-797.

[27] Rehse, S.J. *In Laser-Induced Breakdown Spectroscopy Theory and Applications*, Musazzi, S.; Perini, U., Eds; Springer Series in Optical Sciences 182; Springer: New York, **2014**, 457-484.

[28] Derriger, G.; Suich, R. Simultaneous Optimization of Several Response Variables. *J. Qual. Technol.* **1980**, 12, 214-219.

[29] Gnanamoorthy, P.; Karthikeyan, V. ; Prabu, V.A. Field emission scanning electron microscopy (FESEM) characterisation of the porous silica nanoparticulate structure of marine diatoms*. J. Porous. Mater.* **2013,** 2, 225–233.

[30] De Giacomo, A.; Dell'Aglio, M.; De Pascale, O.; Longo, S.; Capitelli, M. Laser induced breakdown spectroscopy on meteorites. *Spectrochim. Acta, Part B*. **2007**, 62, 1606–1611.

[31] Praher, B.; Palleschi, V.; Viskup, R.; Heitz, J.; Pedarnig, J.D. Calibration free laser-induced breakdown spectroscopy of oxide materials, *Spectrochim. Acta, Part B.* **2010**, 65, 671–679.

[32] Pasquini, C.; Cortez, J.; Silva, L. M. C.; Gonzaga, F. B. Laser Induced Breakdown Spectroscopy. *J. Braz. Chem. Soc.* **2007**, 18 (3), 463-512.

Table 1. Matrix of experiments showing the variables evaluated for optimizing delay time, gate width and laser pulse energy in LIBS determinations. The overall desirability (OD) was used as experimental response.

Experiment		Delay time (ns)		Gate width (ns)		Energy (mJ)		OD
		Real	Coded	Real	Coded	Real	Coded	
Full factorial design 2^3	1	300	-1	1000	-1	45	1	0.20
	2	300	-1	1000	-1	25	-1	0.20
	3	300	-1	3000	1	45	1	0.37
	4	300	-1	3000	1	25	-1	0.84
	5	1500	1	1000	-1	45	1	0.65
	6	1500	1	1000	-1	25	-1	0.72
	7	1500	1	3000	1	45	1	0.88
	8	1500	1	3000	-1	25	-1	0.91
Central point	9	900	0	2000	0	35	0	0.62
	10	900	0	2000	0	35	0	0.61
	11	900	0	2000	0	35	0	0.60
	12	900	0	2000	0	35	0	0.67
	13	900	0	2000	0	35	0	0.62
Axial point	14	10	-1.49	2000	0	35	0	0.00
	15	1910	1.68	2000	0	35	0	0.87
	16	900	0	320	-1.68	35	0	0.43
	17	900	0	3680	1.68	35	0	0.74
	18	900	0	2000	0	22.5	-1.68	0.62
	19	900	0	2000	0	50	1.68	0.58

Table 2.- Spectral lines of the Antarctic soils employed in CF-LIBS. In bold, the lines relevant to both analysis.

Species	Lines wavelength (nm)	
	1st analysis	2nd analysis
Al I	308.20, **309.29**, 394.41	305.71, **309.29**, 396.15
Ba II	-	493.41
Ca I	428.95, 430.73, **431.86**, **443.50**, 526.23, 526.44, 526.98, 558.85 559.42, 612.25, 616.27, 646.24, 649.33	428.30, **431.86**, **443.50**, 445.48, 487.81
Ca II	**315.89**, 317.96, 370.62	**315.89**, 373.72
Cr I	-	357.87, 425.44
Fe I	299.44, 356.99, 361.87, **373.49**, 374.54, **374.95**, 382.02, **404.58** 406.36, 407.16, **432.58**, 440.44	358.12, **373.49**, **374.95**, **404.58**, **432.58**, 438.35, 441.51
Fe II	239.55, 241.12, **241.33**, 257.77, 258.25, 258.58, 260.69, **261.19** **261.38**, 262.83, 271.42, **273.96**, 274.30, 298.48	238.86, **241.33**, **261.19**, **261.38**, 261.76, **273.96**
K I	**766.48**, **769.88**	**766.49**, **769.90**
Li I	-	670.78
Mg I	**517.27**, **518.41**	516.73, **517.27**, **518.41**
Mg II	**279.80**	279.08, **279.80**, 280.27
Mn I	-	403.08, 404.14
Na I	588.95, **589.59**, **819.48**	**589.59**, **819.48**
Si I	**250.69**, **251.61**, **251.92**, **288.16**, 390.56	**250.69**, 251.43, **251.61**, **251.92**, 252.41, **288.16**
Si II	**634.71**	**634.71**, 637.14
Sr I	-	460.73
Sr II	-	407.77
Ti I	498.13, 499.91	500.72, 501.42, 506.47
Ti II	316.84, 321.69, 336.10, **337.28**, 337.99, 338.37, 349.12, 444.34	332.29, **337.28**, 368.52
V I	-	411.18, 411.52, 437.92, 438.99
Zr I	-	468.78
Zr II	-	343.82

Table 3.- Temperature and electronic density values of the campaign 2017/18 samples and the six samples of the campaign 2018/19.

Sample	Tª (K)	Ne (cm^{-3}) × 10^{17}
Soil 2017/18	11294 ± 213	2.49 ± 0.32
PF	8984 ± 53	0.92 ± 0.02
PD	9078 ± 102	0.79 ± 0.01
DB	8971± 57	0.83± 0.02
CG	9005 ± 29	0.83 ± 0.02
PP	9045± 62	0.81 ± 0.02
PL	9063± 22	0.78 ± 0.00

Table 4.- Major oxides in the samples provide by CF-LIBS. The soil sample 2017/18 were analyzed also by ICP-OES to evaluate the CF-LIBS results. The labels correspond to the name of the samples: Playa Fumarolas (PF), Punta Descubierta (PD), Depósito Balleneros (DB), Captador Grande (CG), Pingüinera Punta (PP) and Playa Lobera (PL).

Oxides (%)	PF	PD	DB	CG	PP	PL	Soil sample 2017/18	ICP-OES Soil 2017/18
SiO_2	46.3 ± 5.0	52.7± 5.1	54.9 ± 1.2	50.4 ± 1.9	51.3 ± 2.8	49.3 ± 2.7	34.7 ± 2.7	52.9 ± 0.5
Al_2O_3	19.1 ± 1.7	18.2 ± 1.8	17.2 ± 0.8	19.4 ± 0.6	18.9 ± 2.0	20.9± 1.4	15.5 ± 1.6	16.9 ± 0.2
Fe_2O_3	11.8 ± 1.4	9.9 ± 1.4	9.0 ± 0.2	9.7 ± 0.3	9.8 ± 0.7	10.9 ± 0.6	11.9 ± 1.7	9.3 ± 0.2
CaO	9.0 ± 1.3	7.7± 1.2	7.3 ± 0.5	8.1 ± 1.0	8.2 ± 0.8	7.0 ± 0.9	9.7 ± 1. 5	8.8 ± 0.1
MgO	5.8 ± 1.9	5.0 ± 1.2	4.5 ± 0.5	4.9 ± 0.2	4.1 ± 0.3	4.3 ± 0.6	3.2 ± 0.8	4.7 ± 0.1
Na_2O	3.8± 0.6	3.0 ± 0.4	3.5 ± 0.1	3.4 ± 0.4	4.0 ± 0.3	3.2 ± 0.4	1.9 ± 0.2	4.4 ± 0.0
TiO_2	3.3 ± 0.3	2.6 ± 0.4	3.1 ± 0.2	3.4 ± 0.4	3.1 ± 0.3	3.6± 0.4	3.2 ± 0.3	1.7 ± 0.0
K_2O	1.0 ± 0.2	0.9 ± 0.4	0.7 ± 0.0	0.7 ± 0.1	0.7 ± 0.1	0.8 ± 0.1	0.7 ± 0.1	0.5 ± 0.2

Table 5.- Minority elements concentration of the Antarctic campaign 2018/19 samples provided by LIBS-CL and minority elements concentration of the soil sample 2017/18 determined by ICP-OES. The labels correspond to the name of the samples: Playa Fumarolas (PF), Punta Descubierta (PD), Depósito Balleneros (DB), Captador Grande (CG), Pingüinera Punta (PP) and Playa Lobera (PL).

Elements (g/kg)	PF	PD	DB	CG	PP	PL	ICP-OES soil 2017/18
Mn	5.2 ± 1.7	2.9 ± 0.9	3.6 ± 0.9	3.7 ± 1.1	1.3 ± 0.5	2.7 ± 0.6	1.1
Cr	2.5 ± 1.1	1.8 ± 0.8	2.1 ± 0.9	2.1 ± 0.4	0.6 ± 0.3	2.2 ± 0.8	0.04
V	0.9 ± 0.4	1.2 ± 0.4	1.3 ± 0.7	0.5 ± 0.3	0.6 ± 0.2	1.3 ± 0.3	0.2
Sr	0.5 ± 0.2	0.3 ± 0.1	0.3 ± 0.1	0.3 ± 0.0	0.3 ± 0.0	0.2 ± 0.1	0.4
Zr	0.2 ± 0.1	0.2 ± 0.1	0.2 ± 0.1	0.2 ± 0.1	0.2 ± 0.1	0.2 ± 0.1	0.2
Ba	0.08 ± 0.04	0.04 ± 0.01	0.04 ± 0.01	0.04 ± 0.01	0.04 ± 0.01	0.06 ± 0.01	0.08
Li	0.02 ± 0.01	0.01 ± 0.00	0.01 ± 0.00	0.01 ± 0.00	0.01 ± 0.00	0.01 ± 0.00	0.01

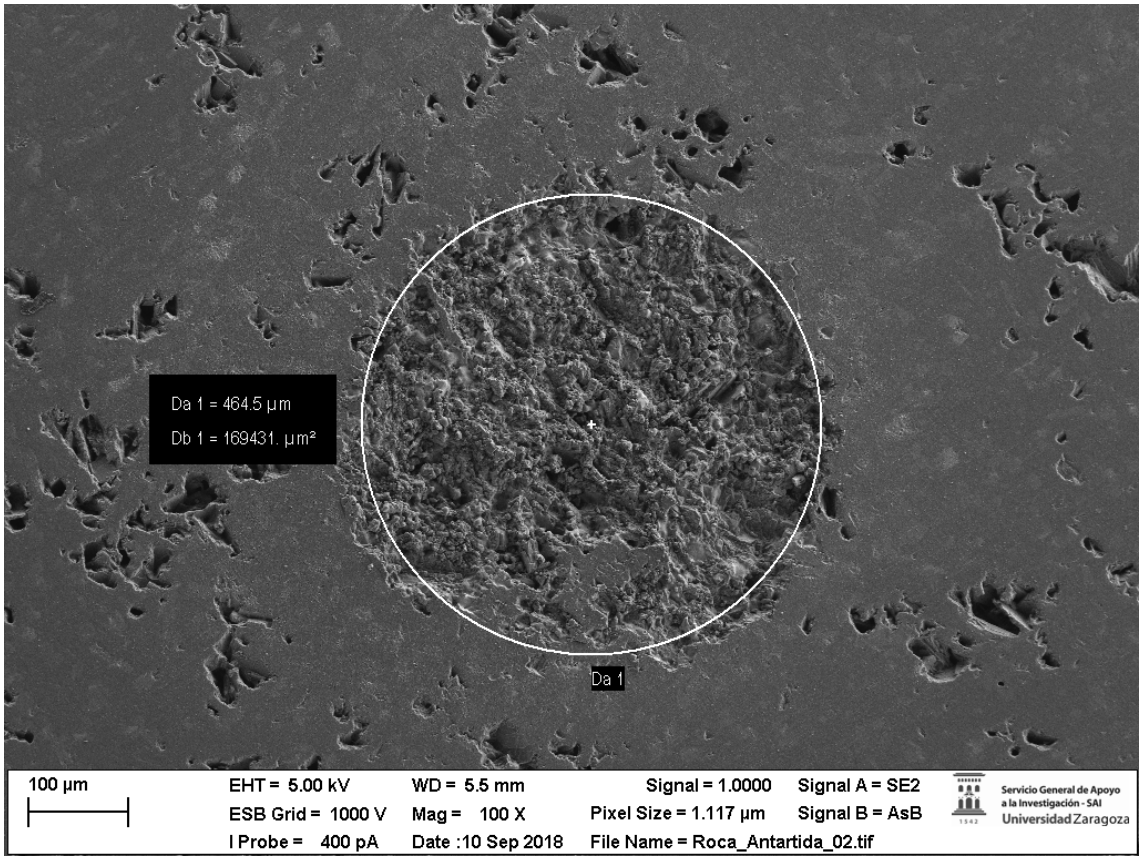

Figure 1.- Nd:YAG laser crater in Antarctic soil sample

1

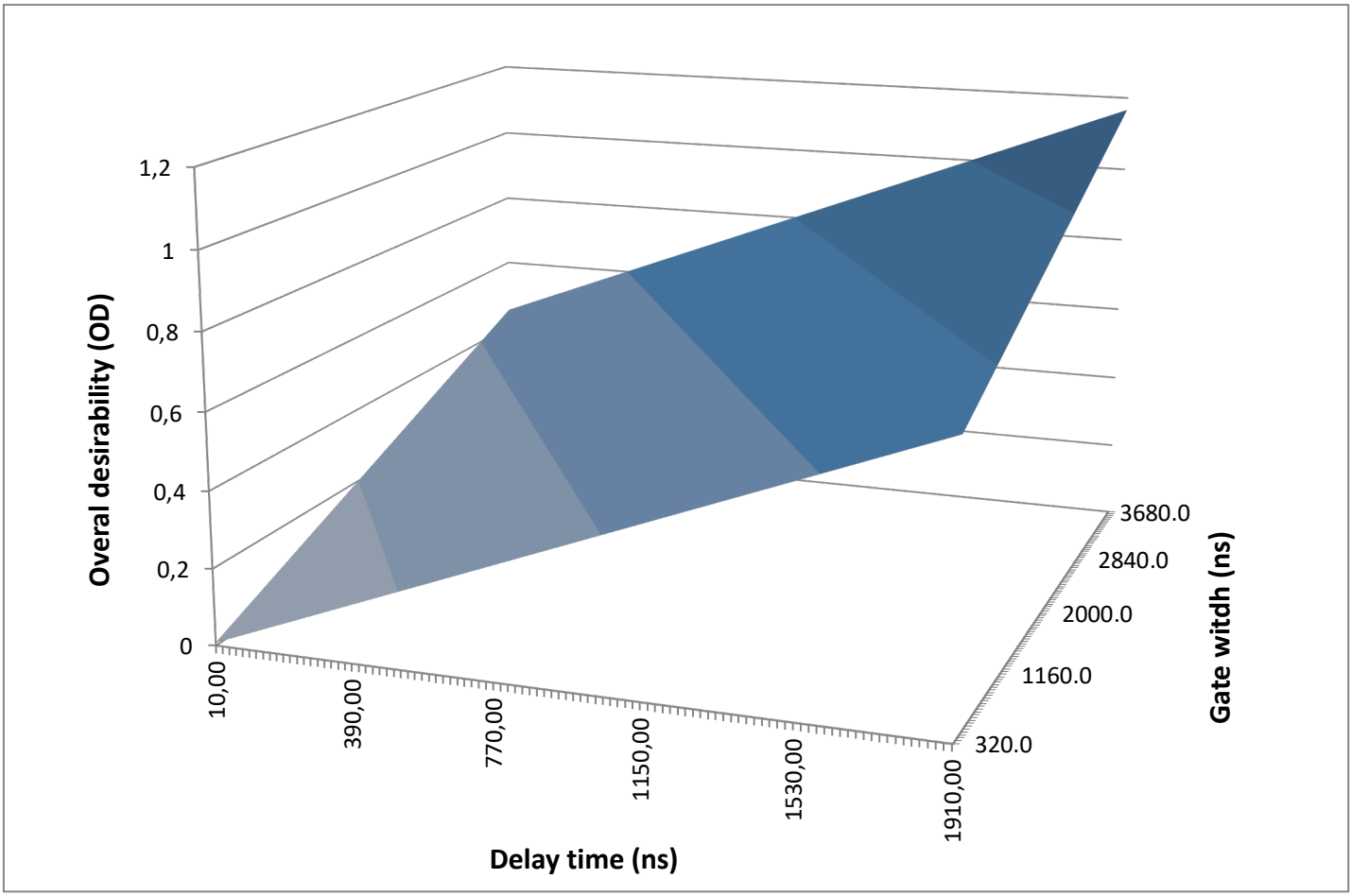

2

3 **Figure 2**.- Response surface for overall desirability (OD) in function of the instrumental
4 parameters: delay time and gate width. The darker areas are the areas with a higher OD.

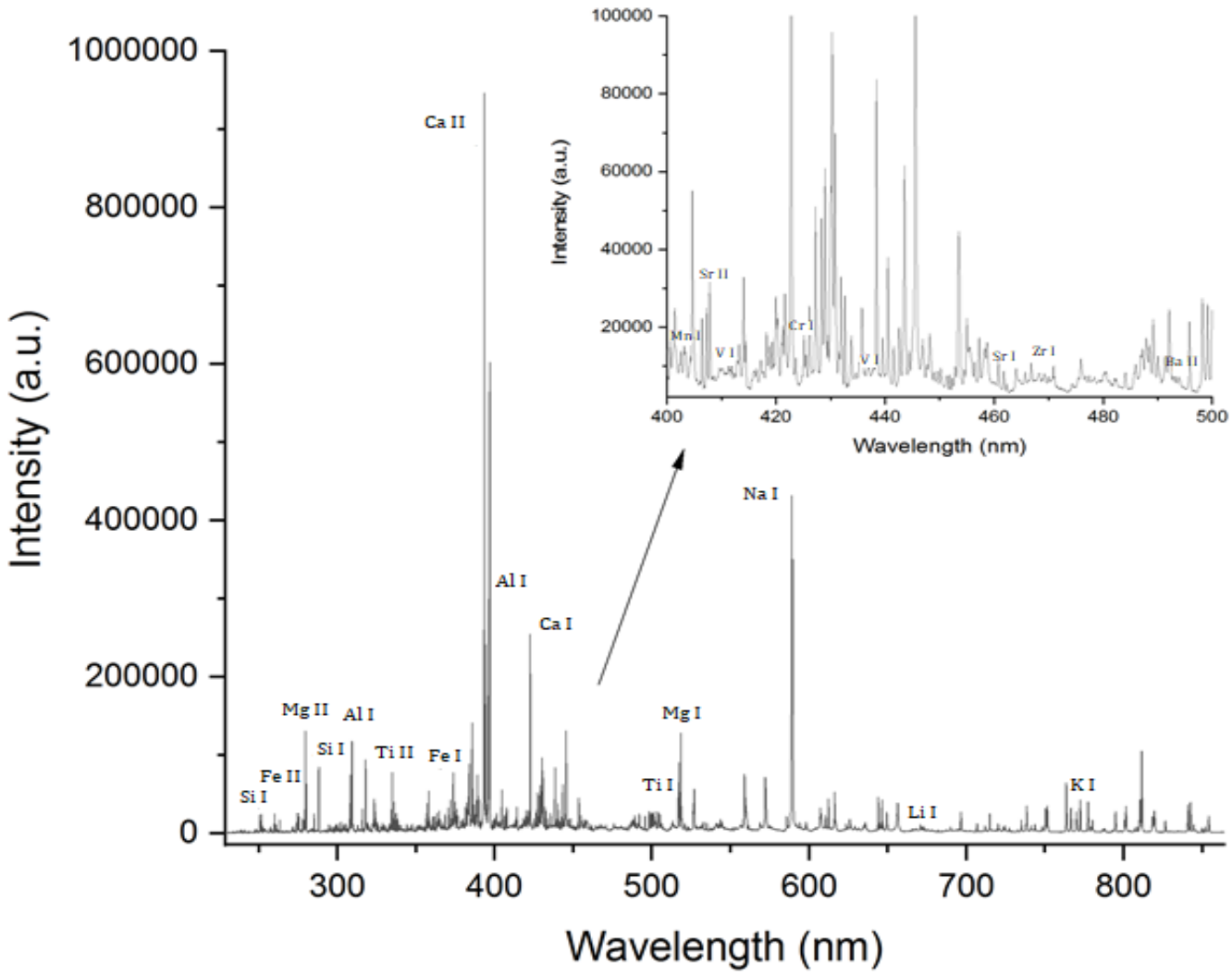

Figure 3.- LIBS spectrum of the Playa Fumarolas sample. Some trace element detection is shown in the inset.

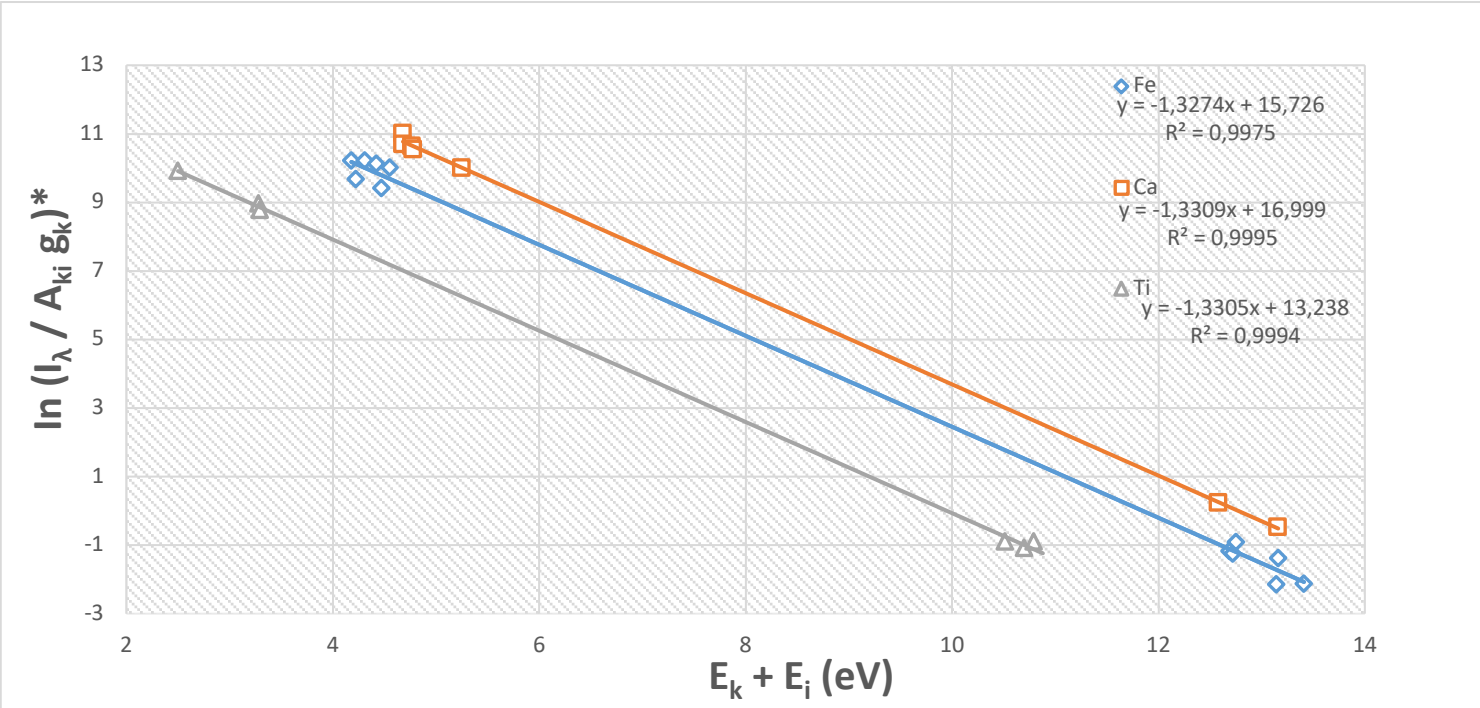

Figure 4.- Saha-Boltzmann plot of the Playa Fumarolas sample created with the spectral lines of Fe, Ca and Ti.